COBEM 2023 27TH INTERNATIONAL CONGRESS OF MECHANICAL ENGENEERING

ABCM Brazilian Society of Mechanical Sciences and Engineering
27th ABCM International Congress of Mechanical Engineering
December 04-08, 2023, Florianópolis-SC, Brazil

COB-2023-0360
TRANSIENT MODELING FOR THE ENERGY CONSUMPTION PREDICTION IN A PORTABLE REFRIGERATOR

Luis Guilherme Fonseca Franco
Guilherme Borges Ribeiro
Aeronautics Institute of Technology, Praça Marechal Eduardo Gomes, São José dos Campos, Brazil
luis.franco@ga.ita.br
gbribeiro@ita.br

Abstract. *The energy consumption in refrigerators can be relatively easily calculated by considering the system's stationary behavior through the balance of mass and energy. However, this analysis proves to be simplistic when attempting to predict consumption closer to reality, as it fails to account for any system failures or sudden changes, causing it to transition from a steady state to transient state. This can occur simply by opening the refrigerator door. Moreover, in real situations, refrigerators do not constantly operate in a steady state as it would lead to excessive consumption and energy demand. Instead, they operate in time cycles, seeking to maintain temperatures close to those desired by the user. Thus, in order to develop an analysis that is useful in practical terms, and optimize energy consumption in real applications, it is necessary to model the cooling system in a way that does not keep it active for long periods of time, as this does not match reality and does not provide acceptable results for energy consumption. Energy consumption tests are time consuming, and a manner to decrease the time and cost in the product development phase is to predict properly an energy consumption test using well-knowm parameters that could be extracted fro a pull-down test. To study energy thermal conductance of heat exchangers, cabinet and compressor. This work aims to carry out this modeling using the Python programming language primarily, which will enable simulations and production of consumption graphs, using the experimental data. The obtained graphs will allow for the analysis of the temperatures of all components of the refrigeration system as well as the cabinet, as function of the time cycles.*

Keywords: *transient state, time cycles, transient modeling.*

1. INTRODUCTION

Refrigeration systems play a crucial role in our daily lives, especially in the context of refrigerators. Understanding the energy consumption of these systems is essential for optimizing their performance and minimizing environmental impact. Traditional approaches to calculating energy consumption rely on steady-state analyses, which oversimplify the complexities of real-world scenarios.

In reality, refrigerators often operate in a transient state due to system failures, sudden changes, or simply the act of opening the refrigerator door. Additionally, continuous operation in a steady state would lead to excessive energy consumption and demand. To bridge the gap between theoretical calculations and practical applications, a more realistic modeling approach is necessary.

Studies of (C Melo and Negrao, 1988), (M J P Janssen and de Wit, 1988) and (Chen and Lin, 1991) presented first principle models to simulate the transient behavior of domestic refrigeration systems aiming at the evaluation of significant variable changes taking place at the system start-ups. Despite the good agreement in steady-state, comparisons with experimental data showed that the actual transient response of the system is not adequately represented by simulation. Moreover, conducting energy consumption tests can be a time-consuming endeavor. However, in order to streamline the product development phase and mitigate expenses, an efficient strategy in accurately predicting energy consumption tests. This can be achieved by utilizing well-established parameters derived froam a pull-down test in a transient simulation approach that predicts the equipment behavior under an on-off control of the temperature cabinet.

The study draws inspiration from various related research. Notably, Andrade et al.'s work (Andrade and Negrão, 2013a) focused on startup tests for household refrigeration systems, proposing online test result predictions. Tagliafico et al. (Tagliafico *et al.*, 2012) presented a compact dynamic model for household vapor compression refrigerated systems, offering valuable insights into system behavior. Borges et al. (Borges *et al.*, 2011) introduced a semi-empirical quasi-steady approach to transient simulation of household refrigerators. Hermes et al. (Hermes *et al.*, 2009) studied energy consumption prediction via steady-state simulation, contributing to energy efficiency efforts.

In addition to these, Subhanjan Bista's research (S Bista, 2018) explored phase change materials to enhance refrigeration system performance and reduce energy consumption. Fangzhou Guo's work (F Guo, 2023) focused on real-time energy performance benchmarking for electric vehicle air conditioning systems using adaptive neural networks and Gaus-

sian process regression. Wei-Jiang Zhang (W J Zhang, 2011) investigated systems with rapid cycling compressors and multi-indoor units, studying air conditioner transient behavior.

The study's significance is further strengthened by Fatemeh Ghadiri's research (F Ghadiri, 2014), which examined the impact of selecting suitable refrigeration cycle components on energy consumption optimization in household refrigerators. Erik Bjork (E Bjork, 2006) explored the performance of domestic refrigerators under varying conditions, such as expansion device, refrigerant charge, and ambient temperature, aligning with the findings of Jasmin Geppert's study (J Geppert, 2013), which analyzed influential factors affecting domestic refrigerators' energy consumption during everyday use.

Considering this aspects, this study introduces a novel modeling approach that aims to mimic real-world operation of refrigeration systems. The proposed approach involves activating the refrigeration system until the ambient temperature reaches a value close to the desired temperature set by the user. Once the desired temperature is achieved, the system is deactivated, remaining idle until the temperature slightly rises. At that point, the system is reactivated to bring the temperature back to the desired level. This cyclic operation accurately reflects the behavior of refrigeration systems in practical applications.

To investigate the energy consumption in this time-cycled format, the study employs transient modeling using the Python programming language. By inputting data regarding the cabinet to be cooled and the compressor utilized in the refrigeration system, the model generates simulations and consumption graphs. These graphs provide insights into the temperatures of all system components and the cabinet over time cycles.

To validate the proposed modeling approach, the results obtained from Python simulations will be compared with those obtained using the EES software (Engineering Equation Solver) and with experimental procedures. By examining the agreement between the various approaches, this study seeks to enhance our understanding of refrigeration system performance and optimize energy consumption in real-world applications.

2. METHODOLOGY

The Mobile Cooling device, which is a compact domestic refrigeration compartment, depicted in the Figure 1, features a vapor compression system that has been modeled. This system consists of a compressor, condenser, expansion device, internal heat exchanger, and evaporator. The corresponding components are illustrated in the Figure 2.

Figure 1. Mobile Cooling device

A numerical approach was undertaken by developing a computational code in the Python programming language (W J Zhang, 2011), utilizing the CoolProp library to acquire the thermodynamic properties.

In the transient phase, the compressor, the condenser and the evaporator were modeled, while the transient stages of the expansion valve was considered negligible compared to the heat exchangers' transient stage (J Geppert, 2013). The heat transfer between the compressor and the environment was taken into account in the calculations. Since our modeling approach incorporates time cycles, distinct calculations were conducted for the operational and non-operational states of the device. The calculation processes are aiming to determine the condensation and evaporation temperatures of the refrigerant fluid over time. To find the solution, initial guesses for both temperatures are used. Subsequently, a target temperature is established for the device, ensuring that the system remains operational until the desired temperature is attained. Once reached, the device is switched off until the temperature increases by $5°C$. At that point, it is turned on again, repeating the cyclic process. Finally, an explicit energy balance is proposed to calculate the temperature for the next time step.

With an initial guess of T_C and T_E, it is possible to determine the following quantities, one by one (Negrão COR, 2011). In the equations displayed here, T represents temperature, while the subscripts 1, 3, 5, sub and sup represent com-

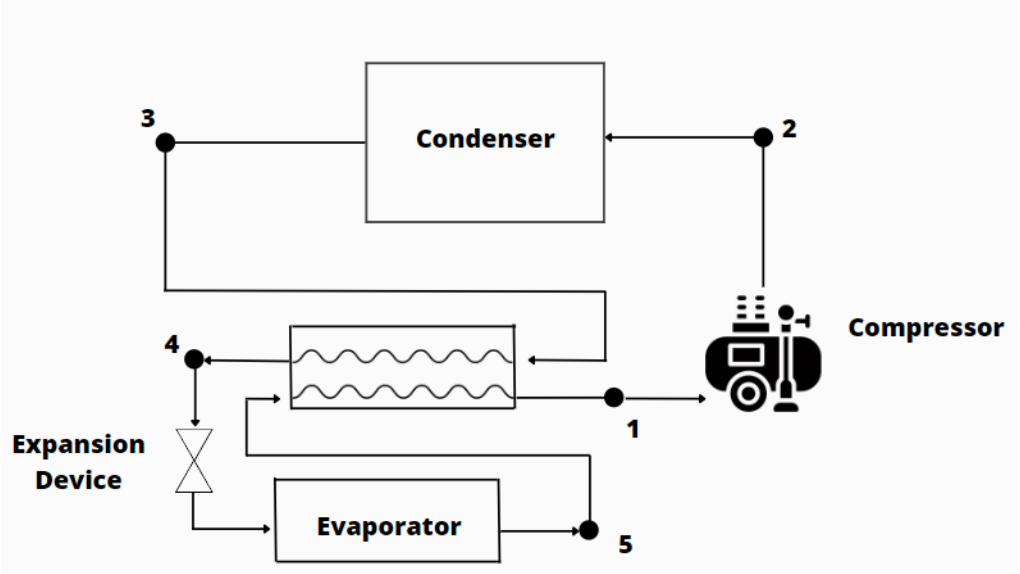

Figure 2. vapor compression system.

pressor inlet, condenser outlet, evaporator outlet, subcooling and superheating, while c represents condenser, e represents evaporator and ϵ represents the effectiveness of the internal heat exchanger:

$$T_3 = T_C - T_{sub}, \tag{1}$$

$$T_5 = T_E + T_{sup}, \tag{2}$$

$$T_1 = T_5 + \epsilon \cdot (T_3 - T_4), \tag{3}$$

The approach described above, which assumes fixed superheating and sub-cooling degrees at the outlet of the heat exchangers, has been utilized in previous studies involving refrigerants (Negrão COR, 2011) (Ribeiro and Barbosa, 2018) (J M Gonçalves, 2011) (Ribeiro and Barbosa, 2016). This method offers a significant advantage of bypassing complexities associated with modeling expansion devices.

The aforementioned temperatures were employed to assess the thermophysical properties of each fluid, considering specific condensation and evaporation pressure values. In terms of the compressor, it was modeled utilizing the following equations to determine the enthalpy at the discharge of the compressor:

$$\dot{W} = \dot{m} \cdot (h_{2s} - h_1)/\eta_G, \tag{4}$$

In the equation, $\dot{W}$ denotes the compressor power, $\dot{m}$ represents the mass flow rate of the fluid, h_1 signifies the specific enthalpy at the compressor inlet, h_{2s} indicates the specific enthalpy at the compressor discharge in an isentropic process transitioning from h_1 at the evaporator pressure to h2 at the condenser pressure, and η_G represents the overall efficiency of the compressor.

By assuming initial values for the condenser and evaporator temperatures at time t = 0, it is possible to compute the temperature in the subsequent time step. This is achieved through an energy balance applied to the condenser, considering a given T_C (condensation temperature), as well as energy balances on both evaporators. These calculations are followed by a refrigerant mass flow balance. To determine the temperature in the next time step for the condenser, the following equation can be utilized, as showed in the recent work (Andrade and Negrão, 2013b):

$$\frac{C_C \cdot (T_C - T_{C0})}{dt} = \dot{m} \cdot (h_2 - h_3) - UA_C \cdot (T_{C0} - T_{amb}), \tag{5}$$

Where C is the heat capacity, T_C is the temperature in the condenser exit, UA_C is the condenser conductance and $\dot{m}$ is the mass flow rate. Similarly, for the evaporator, the compressor and the device, the energy balance is given by:

$$\frac{C_{comp} \cdot (T_2 - T_{20})}{dt} = \dot{m} \cdot (h_2 - h_1) - UA_{comp} \cdot (T_2 - T_{amb}) + \dot{W}, \tag{6}$$

$$\frac{C_E \cdot (T_E - T_{E0})}{dt} = -\dot{m} \cdot (h_1 - h_3) + UA_E \cdot (T_{RFR} - T_{E0}), \tag{7}$$

$$\frac{C_{gab} \cdot (T_{gab} - T_{gab0})}{dt} = UA_{gab} \cdot (T_{amb} - T_{gab0}) - UA_E \cdot (T_{RFR} - T_{E0}), \tag{8}$$

The calculations were conducted using the refrigeration fluid studied in this work, namely R-600a. The obtained values for condensation, evaporation, and mass flow rate were utilized to analyze the system's behavior over time.

This numerical procedure begins by setting the ambient temperature as the initial value for all components. Next, the known parameters are specified, and the desired temperature for the cabinet is defined. After that, the system is activated, and the temperatures of each component are calculated for each time-step using the equations 5, 6, 7 and 8, through a fully explicit approach . These temperature values are then stored in temperature vectors.

Once the system temperature falls below $2°C$ compared to the desired temperature, the system is switched off and remains idle until the cabinet temperature increases by $2°C$ above the desired level. During this period of system inactivity, the same approach as mentioned earlier is employed to calculate the temperature over time. It assumes that the compressor has zero rotation, implying $\dot{m} = 0$. Once the temperature reaches this threshold, the system is reactivated, and the entire process is repeated for a predetermined duration.

3. RESULTS AND DISCUSSION

The data input was obtained mostly by a pull-down test provided by Embraco, non-linear regression was conducted to obtain the conductance and heat capacity values of the components, using the least squares method. By conducting the pull-down test, the system component temperatures were recorded over time, enabling the determination of thermodynamic properties for each time interval. Subsequently, nonlinear combinations of component conductance and thermal capabilities were modeled as functions as showed an example in the equation 9, for the condenser. Through the EES software, the method of least squares was utilized to iteratively approximate the parameters and obtain the optimal values that minimize the σ value, assuming $y'(i) = 0$. The values are shown in Table 1.

$$y(i) = \frac{C_C \cdot (T_C(i) - T_{C0}(i))}{dt} - \dot{m}(i) \cdot (h_2(i) - h_3(i)) + UA_C \cdot (T_{C0}(i) - T_{amb}(i)), \tag{9}$$

$$\sigma = \sum_{n=1}^{N} (y'(i) - y(i))^2, \tag{10}$$

Table 1. Input data for the mathematical model.

Input Name	Simbol	Value	Unit
External Temperature	T_{amb}	32	$[°C]$
Desired Cabin Temperature	T_{gab}	5	$[°C]$
Reference Volume	V_{ref}	26E-8	$[m^3]$
Compressor Rotation	ROT	340	$[Hz]$
Sub cooling	T_{sub}	3	$[°C]$
Super heating	T_{sup}	3	$[°C]$
Internal HX effectiveness	ϵ	0.8	[-]
Compressor conductance	UA_{comp}	130.52	$[W/K]$
Condenser conductance	UA_C	10.11	$[W/K]$
Evaporator conductance	UA_E	9.99	$[W/K]$
Cabin conductance	UA_{gab}	0.5	$[W/K]$
Compressor heat capacity	C_{comp}	0.744	$[J/K]$
Condenser heat capacity	C_C	987.77	$[J/K]$
Evaporator heat capacity	C_E	948.77	$[J/K]$
Cabin heat capacity	C_{gab}	1063.47	$[J/K]$
Time step	dt	1	$[s]$

The test was carried out for ambient temperatures of 25 $°C$, $32°C$ and $43°C$. The presented Figures 3, 4 and 5 exhibits the temporal evolution of the compressor, condenser, evaporator, and cabin temperatures throughout a simulation lasting 1500 seconds, for the ambient temperatures of 25 $°C$, $32°C$ and $43°C$ respectively.

Upon conducting a meticulous analysis of these graphs, it becomes evident that the behavior of temperatures in all three cases exhibits a striking similarity, aligning precisely with our initial expectations. The data reflects a consistent and predictable pattern, affirming the reliability of the model's simulations.

Furthermore, a thorough examination allows for the verification that the cabinet temperature remains remarkably close to the desired value across all three scenarios. The range of oscillation, fluctuating between $3°C$ and $7°C$, demonstrates a

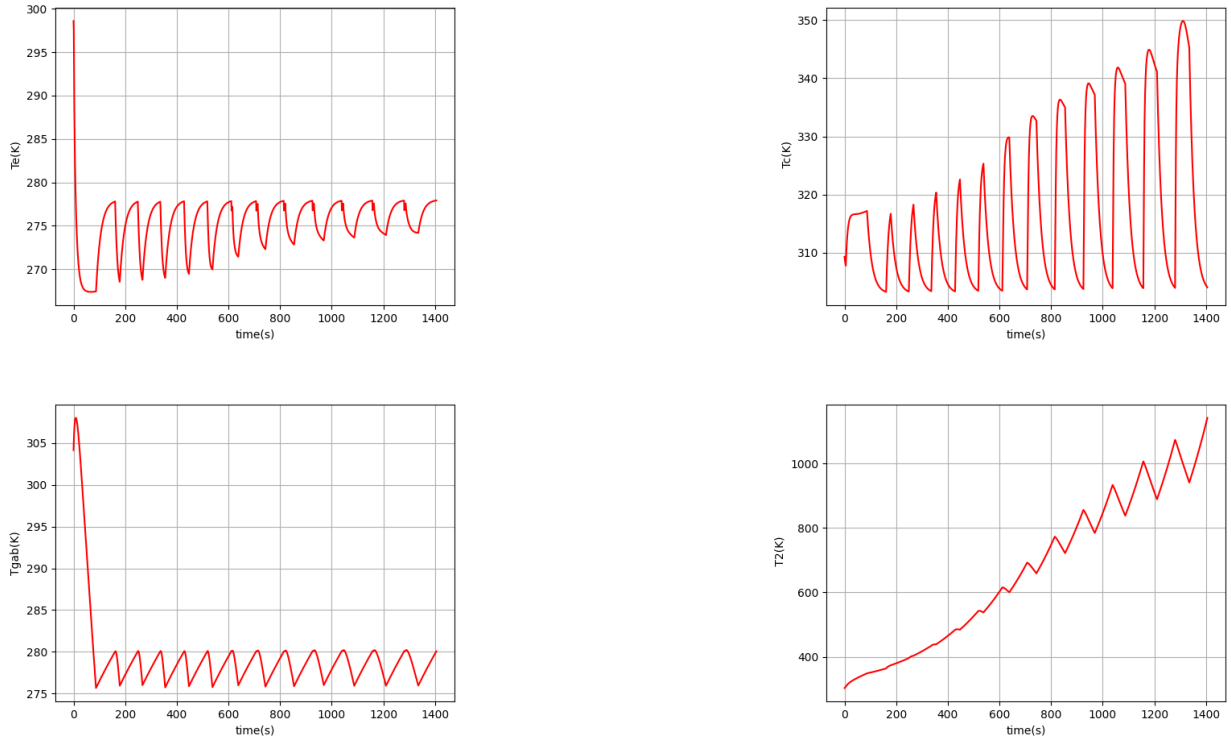

Figure 3. Temperatures over time for $T_{amb} = 25°C$.

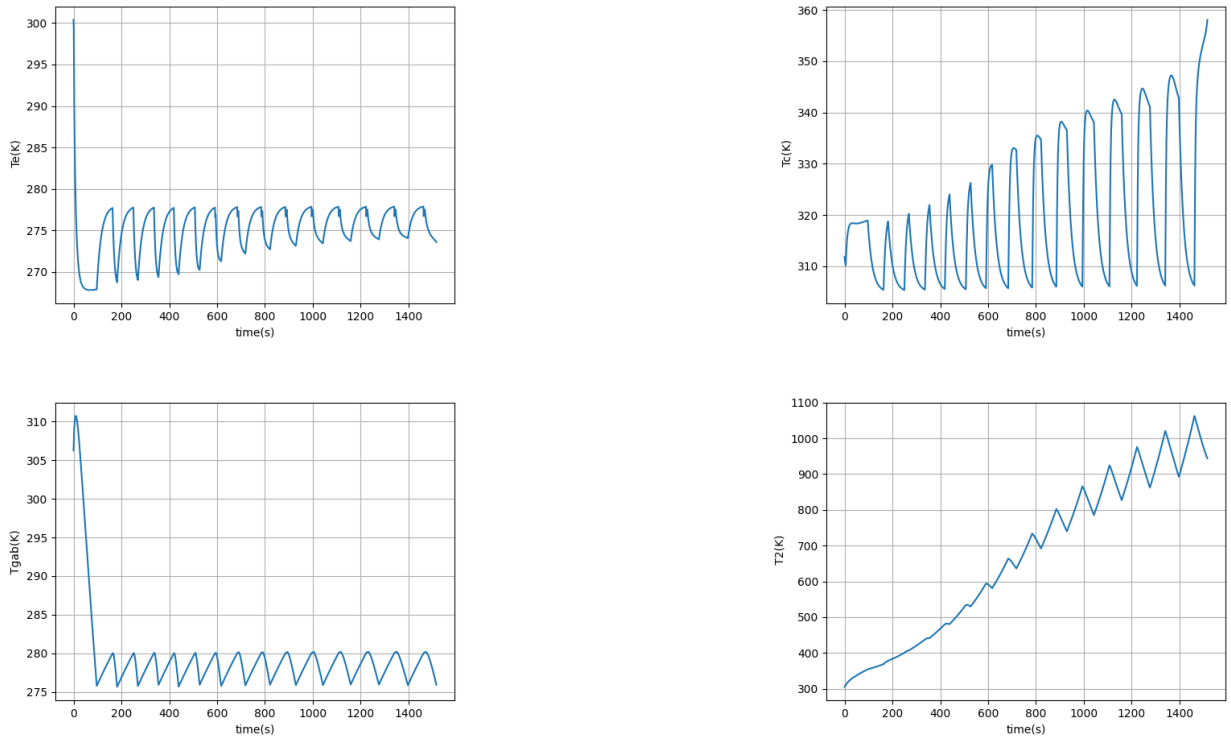

Figure 4. Temperatures over time for $T_{amb} = 32°C$.

commendable level of stability and adherence to the expected parameters. This observation reinforces the notion that the model's proposal of simulating an on-off regime to optimize energy consumption is well-founded and aligns with industry best practices.

Taking the ambient temperature of 32 $°C$ as a representative instance, as depicted in Figures 4 and 7, we can observe a

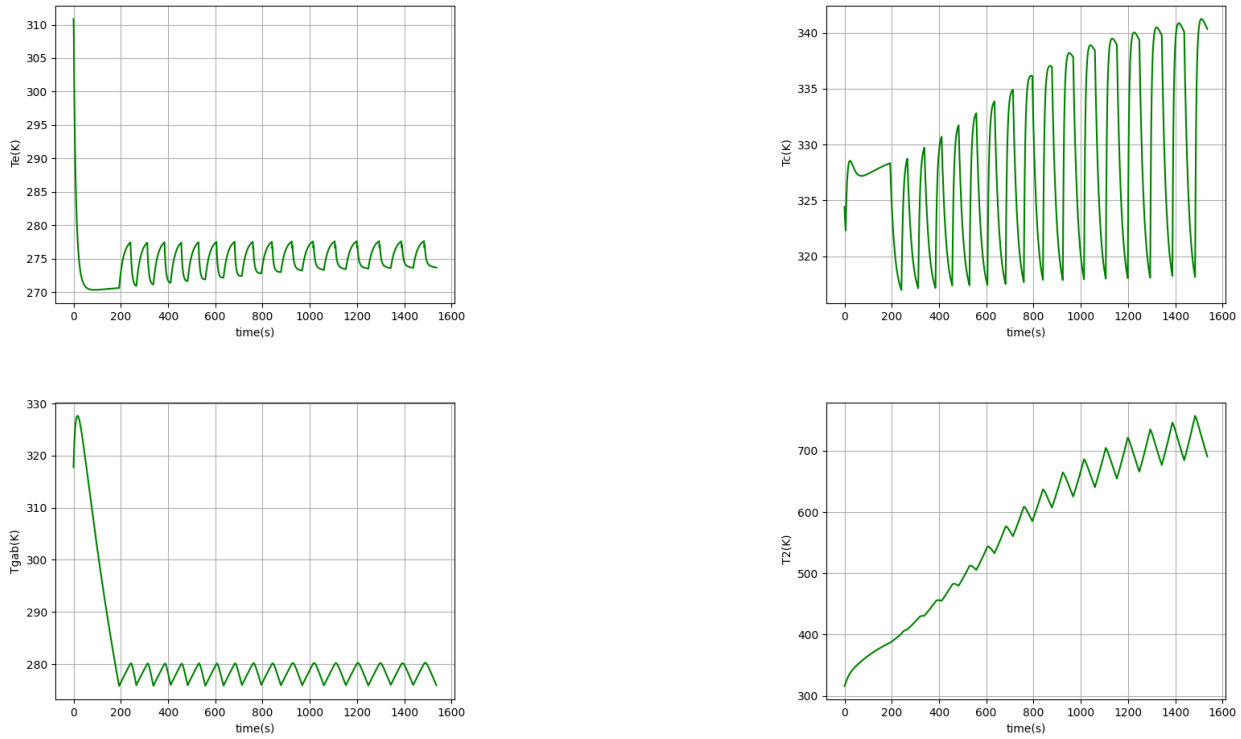

Figure 5. Temperatures over time for $T_{amb} = 43°C$.

swift and conspicuous drop in the cabinet's internal temperature during the initial system activation. This decline persists until it reaches 2 $°C$ below the desired temperature. At this critical point, the system automatically turns off, allowing for the cabinet temperature to increase until it surpasses the desired level by an additional 2 $°C$. This cyclic operational pattern persists throughout the designated time frame, culminating in a temperature equilibrium that closely aligns with the chosen setpoint.

Similar to the cabinet, the evaporator follows a comparable thermal trajectory, with temperature undergoing a steep and similar drop during the initial moments of system operation. This mirrored temperature pattern is a direct result of the rapid and consequential state transition occurring within the system. The evaporator, initially exposed to ambient temperature, undergoes a significant shift when the system is activated, leading to a sudden temperature decrease. This temperature decrease continues until the evaporator reaches the operational temperature, at which point a gradual increase follows, eventually stabilizing when the system is deactivated.

It is important to note that the oscillations in the evaporator's temperature profile diminish over time. This temporal reduction in oscillations stems from the consistent rise in operational temperature, resulting from the energy contributions produced by compressor-driven activities. Similarly, the temperature at the condenser outlet follows a similar trajectory, with an immediate and marked increase upon system activation. This temperature increase progresses steadily until it aligns with the predefined operational level, maintaining an equilibrium throughout the active phase of the system. Nevertheless, these oscillations gradually intensify over time due to the accumulating heating effect brought by the increase of the temperature at the compressor outlet.

In sharp contrast, the temperature at the condenser inlet was a persistent, and noticeable upward trend during the simulation period. At this point, oscillations are noticeably reduced, a phenomenon attributed to the mitigation of sudden pressure fluctuations. Nonetheless, an important observation is the increasing magnitude of these oscillations over time, consistent with the behavior previously discussed regarding the evaporator and condenser outlet temperatures.

Turning our focus to the compressor speed behavior, it can be observed that its operational cycles consist of brief yet distinct activation periods interspersed with extended periods of dormancy. This inherent operational rhythm aligns well with physical expectations, as the gradual heating mechanism of natural convection lags behind scenarios where substantial pressure differences lead to more rapid and pronounced temperature changes. Additionally, a significant trend emerges over time, with the cumulative operational duration of the compressor extending progressively in parallel with the system's increase in pressure. This elongation induced by the pressure rise results in a gradual reduction of the applied pressure difference, encapsulating the evolving performance dynamics of the compressor.

An examination of the energy consumption graph corroborates this overarching narrative. Clearly, each instance of system activation results in a distinct peak in energy consumption, which is a direct outcome of the substantial pressure

difference during startup. Remarkably, as the operational timeline of the system unfolds, energy consumption gradually decreases in tandem with the diminishing pressure difference.

Moreover, a deeper analysis unveils an intriguing correlation between ambient temperature and the system's response. As the ambient temperature rises, it is possible to observe an increase in the number of on-off cycles performed within a given time period. Simultaneously, the duration of these cycles decreases. This intriguing relationship can be attributed to the system's sensitivity to temperature changes, particularly the rapid temperature increase within the cabinet when the system is in the off state. The model's ability to accurately capture this phenomenon adds further credibility to its validity and underscores its effectiveness in accurately simulating real-world dynamics.

By dissecting the intricacies of these graphs, valuable insights emerge, shedding light on the complex interplay of variables and their impact on temperature dynamics. This comprehensive analysis not only validates the alignment between expected and observed outcomes but also provides a deeper understanding of the system's behavior and performance.

These findings carry significant implications, both in terms of system optimization and energy efficiency. The close resemblance between expected and actual temperature behavior, coupled with the sensitivity to ambient temperature changes, emphasizes the model's ability to adapt and respond to evolving environmental conditions. Such adaptability is crucial in domains where precise control and energy conservation are paramount concerns.

Additionally, the Figures 6, 7 and 8 illustrates the energy consumption and rotational changes over the same durationl, for the ambient temperatures of 25 $^{\circ}C$, 32$^{\circ}C$ and 43$^{\circ}C$ respectively.

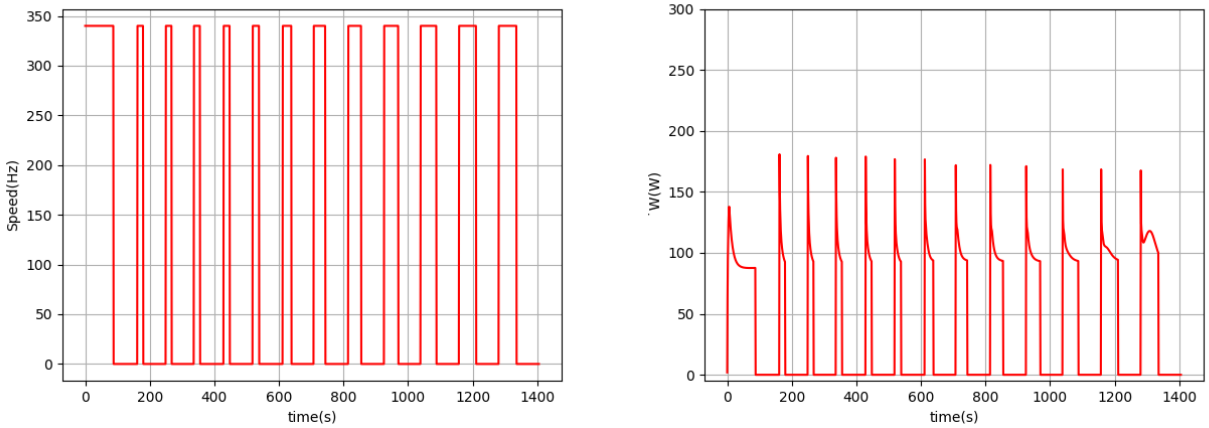

Figure 6. Speed and energy Consumption over time for $T_{amb} = 25^{\circ}C$.

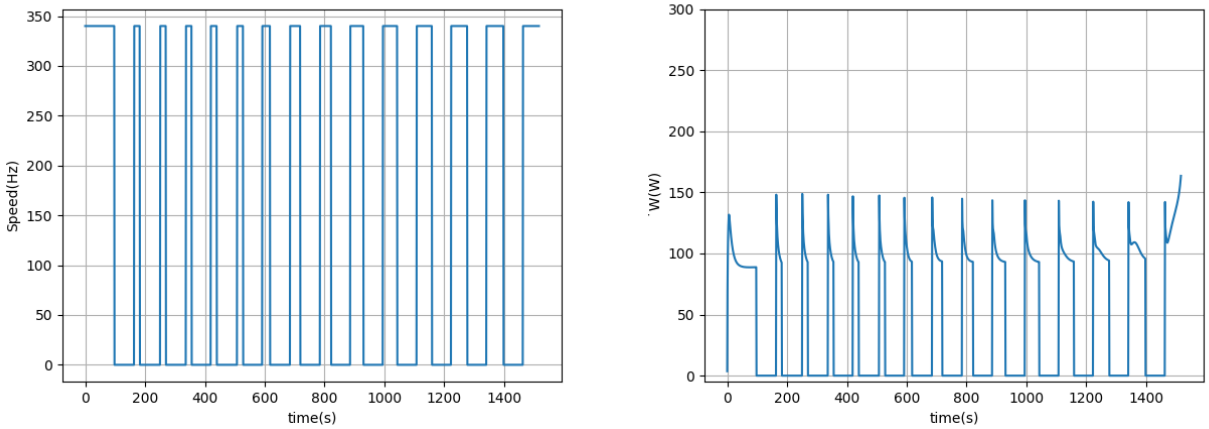

Figure 7. Speed and energy Consumption over time for $T_{amb} = 32^{\circ}C$.

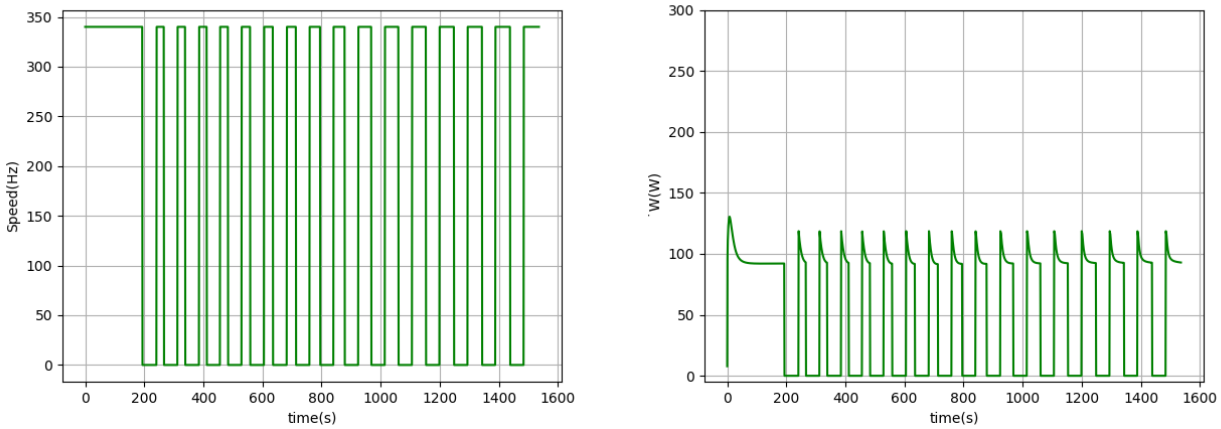

Figure 8. Speed and energy Consumption over time for $T_{amb} = 43°C$.

Upon a meticulous analysis of these graphs, a notable disparity becomes apparent in the duration of the system's operation until reaching a temperature of $3°C$ for the first time. This duration exhibits a consistent increase in tandem with the rise in ambient temperature, aligning precisely with our initial expectations. Such findings shed light on the system's sensitivity to external conditions and provide valuable insights into its performance.

Subsequently, the observed speed and energy comsumption curves manifest the anticipated patterns, showcasing the expected behavior. When the system is operational, the compressor maintains a constant speed, ensuring a stable temperature output. Conversely, during the off state, the compressor comes to a complete halt, resulting in zero rotation. This behavior is in line with the theoretical understanding of the system's operations.

Notably, an intriguing peak in energy consumption accompanies each activation of the system. This peak aligns with the existence of an activation energy inherent in the system, resulting from the rapid transition of the compressor from a state of rest to high RPM. The presence of this energy requirement is consistent with the observed peak in energy consumption, substantiating the accuracy of the model's representation.

Furthermore, it is worth noting that this energy peak diminishes as the ambient temperature rises. This occurrence can be attributed to a decrease in the activation energy. At higher external temperatures, the system remains in the off state for a shorter duration, requiring less energy to initiate the compressor's rotation. This inverse relationship between ambient temperature and energy peak further reinforces the model's credibility in capturing real-world dynamics.

By delving into the intricacies of these graphs, a deeper understanding of the system's behavior and energy consumption patterns emerges. The observed duration disparities, the consistent format of the temperature curves, and the correlation between activation energy and energy peaks provide critical insights into system optimization and energy efficiency considerations.

Displayed in the Table 2 is the comprehensive depiction of the simulation's total energy consumption for all the ambient temperatures. These values are revealing a direct correlation between consumed energy values and ambient temperature. Notably, as the ambient temperature rises, the consumed energy values exhibit a simultaneous increase. This observation aligns harmoniously with our initial expectations and serves as a valuable validation of the model's accuracy.

Table 2. Total energy consumption.

Energy consumption $[J]$	**Ambient temperature** $[°C]$
5.05E4	25
6.25E4	32
7.8E4	43

The parallel rise in consumed energy values and ambient temperature underscores the system's sensitivity to external conditions. As the temperature climbs, the system faces greater challenges in maintaining the desired temperature, necessitating increased energy input. This correlation confirms the model's ability to capture the intricate dynamics between temperature variations and energy consumption.

4. CONCLUSIONS AND FURTHER WORKS

The present study encompasses a numerical analysis of a refrigeration cycle employed in a Mobile Cooling device, operating under vapor compression conditions with the Ra134a fluid. Additionally, a detailed description of the mathematical model utilized is provided, emphasizing its implementation in the transient state and its operation within time

cycles. This investigation focuses on elucidating the temperature variations of the system's components over time, as well as showcasing the total energy consumption, which was a key parameter aimed at minimization.

The simulation duration spanned approximately 25 minutes, underscoring the significance of comprehending the transient behavior of such a system in order to understand its overall functioning. This work's relevance extends beyond academia, as it offers valuable insights for commercial applications, considering the high costs and limitations associated with conventional pool-Down tests that fail to account for cyclic operation.

In future endeavors, it is suggested that alternative models be developed, wherein time cycles are not solely dictated by the cabin temperature variation but rather seek to maintain a constant temperature while modulating the compressor's rotation. Such an approach could further enhance the efficiency and performance of the system.

5. REFERENCES

Andrade, D.E.V. and Negrão, C.O.R., 2013a. "Analysis of start-up tests of household refrigeration systems. a potential for on-line predictions of test results." *Applied Thermal Engineerings*, Vol. 54, pp. 255–263.

Andrade, D.E. and Negrão, C.O., 2013b. *Analysis of start-up tests of household refrigeration systems. A potential for on-line predictions of test results*. Ph.D. thesis, Postgraduate Program in Mechanical and Materials Engineering, Federal University of Technology-Paraná, Curitiba, Brasil.

Borges, B.N., Hermes, C.J.L., Gonçalves, J.M. and Melo, C., 2011. "Transient simulation of household refrigerators: A semi-empirical quasi-steady approach." *Applied Energy*, Vol. 88, pp. 748–754.

C Melo, R T de Silva Ferreira, R.H.P. and Negrao, C.O.R., 1988. "Dynamic behaviour of a vapor compression refrigerator: A theoretical and experimental analysis". *International Refrigeration and Air Conditioning Conference*, pp. 98–106.

Chen, Z.J. and Lin, W.H., 1991. "Dynamic simulation and optimal matching of a small-scale refrigeration system". *International Refrigeration and Air Conditioning Conference*, Vol. 14, pp. 329–335.

E Bjork, B.P., 2006. "Performance of a domestic refrigerator under influence of varied expansion device capacity, refrigerant charge and ambient temperature". *International Journal of Refrigeration*, Vol. 29, pp. 789–798.

F Ghadiri, M.R., 2014. "The effect of selecting proper refrigeration cycle components on optimizing energy consumption of the household refrigerators." *Applied Thermal Engineering*, Vol. 67, pp. 335–340.

F Guo, Z Chen, F.X.A.L.J.S., 2023. "Real-time energy performance benchmarking of electric vehicle air conditioning systems using adaptive neural network and gaussian process regression." *Applied Thermal Engineering*, Vol. 222.

Hermes, C.J.L., Melo, C., Knabben, F.T. and Gonçalves, J.M., 2009. "Prediction of the energy consumption of household refrigerators and freezers via steady-state simulation." *Applied Energy*, Vol. 86, pp. 1311–1319.

J Geppert, R.S., 2013. "Analysis of effecting factors on domestic refrigerators' energy consumption in use". *Energy Conversion and Management*, Vol. 76, pp. 794–800.

J M Gonçalves, Melo C, H.C.B.J., 2011. "Experimental mapping of the thermodynamic losses of vapor compression refrigeration systems." *Journal of the Brazilian Society of Mechanical Sciences and Engineering*, Vol. 34, pp. 159–165.

M J P Janssen, L.J.M.K. and de Wit, J.A., 1988. "Theoretical and experimental investigation of a dynamic model for small refrigerating systems". *International Refrigeration and Air Conditioning Conference*, pp. 245–255.

Negrão COR, H.C., 2011. "Energy and cost savings in household refrigerating appliances: A simulation-based design approach." *Applied Energy*, Vol. 88, pp. 3051–3060.

Ribeiro, G.B. and Barbosa, J.R., 2016. "Analysis of a variable speed air conditioner considering the r-290/poe iso 22 mixture effect." *Applied Thermal Engineering*, Vol. 108, pp. 650–659.

Ribeiro, G.B. and Barbosa, J.R., 2018. "Numerical analysis of r-290/poe iso 22 condensers based on the second law and seer rating." *International Journal of Refrigeration*, Vol. 88, pp. 441–450.

S Bista, S E Hosseini, E.O.G.P., 2018. "Performance improvement and energy consumption reduction in refrigeration systems using phase change material (pcm)." *Applied Thermal Engineering*, Vol. 142, pp. 723–745.

Tagliafico, L.A., Scarp, F. and Tagliafico, G., 2012. "A compact dynamic model for household vapor compression refrigerated systems." *Applied Thermal Engineerin*, Vol. 35, pp. 1–8.

W J Zhang, C.L.Z., 2011. "Transient modeling of an air conditioner with a rapid cycling compressor and multi-indoor units". *Energy Conversion and Management*, Vol. 52, pp. 1043–1061.

6. RESPONSIBILITY NOTICE

The authors are the only responsible for the printed material included in this paper.